



The synthesis of novel, visible-wavelength, oxidizable polymerization sensitizers based on the 8-halogeno-5,12-dihydroquinoxalino[2,3-*b*]quinoxaline skeleton

Radosław Podsiadły*, Agnieszka M. Szymczak, Karolina Podemska

Institute of Polymer and Dye Technology, Technical University of Lodz, Stefanowskiego 12/16, 90-924 Lodz, Poland

ARTICLE INFO

Article history:

Received 14 November 2008

Received in revised form

12 February 2009

Accepted 15 February 2009

Available online 26 February 2009

Keywords:

5,12-Dihydroquinoxalino[2,3-*b*]quinoxaline dyes

Free radical polymerization

Cationic polymerization

Photo-induced electron transfer

ABSTRACT

Novel dyes, based on the 8-halogeno-5,12-dihydroquinoxalino[2,3-*b*]quinoxaline skeleton, were synthesized and characterized using ^1H NMR spectroscopy and chemical ionization mass spectroscopy. Their electrochemical and spectral properties, such as absorption and emission spectra, quantum yield of fluorescence and quantum yield of singlet oxygen generation, were also measured. These dyes were used as oxidizable sensitizers for diphenyliodonium and N-alkoxypyridinium salts. Photoredox pairs, consisting of dyes and pyridinium or iodonium salts, were found to be effective visible-wavelength initiators of free radical or cationic polymerization, respectively. The ability of each dye to act as a photoinitiator strongly depended upon its chemical structure. The heavy atoms present in the chemical structure could lead to excited triplet states within the dye, thereby facilitating electron transfer from these states.

© 2009 Elsevier Ltd. All rights reserved.

1. Introduction

Light-induced photopolymerization has several advantages over other comparable methods. For instance, it is a low-temperature process that can be controlled by manipulating the intensity and wavelength of the radiation source.

Photosensitized polymerization is induced by UV or visible light. These processes have received considerable attention in the last decade and have found wide application in imaging, radiation curing technologies, e.g., inks, photoresists, photolithography, photocurable coatings [1,2]. During UV initiated polymerization, the photoinitiators are directly fragmented into radical species (Scheme 1) that can initiate polymerization of acrylate or multi-acrylate monomers [3]. In cation-induced polymerization reactions, photo-sensitive initiators, commonly diaryliodonium salts, undergo irreversible photofragmentation in response to UV excitation to produce free-radical, cationic, and radical cation fragments. The aryl cations and aryl iodine radical cations, generated from photolysis, further react with either solvent molecules or monomers to generate a strong protic acid, H^+X^- . This acid, in turn, initiates the polymerization of the epoxide monomers. This concept is illustrated in Scheme 2 [3] for the UV-induced ionic fragmentation of an iodonium salt and the subsequent acid formation.

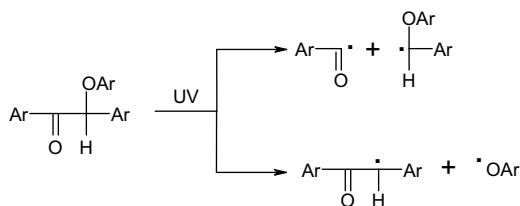
Unfortunately, the onium salts used in photopolymerization primarily absorb wavelengths of light between 225 and 350 nm. In order to extend the spectral sensitivity of these initiators to the visible light, sensitizers are used. The most efficient and generally applicable mechanisms of photosensitization of diaryliodonium [4], triphenylsulfonium [5], and N-alkoxypyridinium [6] salts are photoinduced intermolecular electron transfer processes. In such processes, the photo-excited sensitizer (Dye^*) is oxidized by the salt (X-Y^+) to form a corresponding radical cation ($\text{Dye}^{\bullet+}$) and iodonium/pyridinium salt radical (X-Y^\bullet) that undergoes cleavage as depicted in Scheme 3. The Y^\bullet radical can initiate free radical polymerization reactions, such as the polymerization of an acrylate, whereas the radical cation, $\text{Dye}^{\bullet+}$, can initiate the cationic polymerization of epoxide monomers. Alternatively, the radical cation may interact with solvents or monomers to release strong protic acid, which can initiate cationic polymerization.

There are very few chemicals from which photooxidizable sensitization systems can be prepared. Photosensitizers for acrylate monomers include cyanine [7], coumarin [7], and acridinedione dyes [8]. Cationic polymerization reactions can be initiated by perylene [6], coumarin [9], and curcumin [10] dyes. In cationic initiation, the excited states of the dyes transfer electrons to the onium salts.

The recent studies have revealed that the most efficient sensitizers for pyridinium salt decomposition are fluoquinone dyes [11] and derivatives of 5,12-dihydroquinoxalino[2,3-*b*]pyridopyrazine [12] (especially dyes with “heavy atoms” such as bromine or

* Corresponding author. Fax: +48 42 636 25 96.

E-mail address: radekpod@p.lodz.pl (R. Podsiadły).



Scheme 1.

chlorine). Therefore, the main goals of this study were to synthesize novel dyes (**4a–4f**) based on the 8-bromo- and 8-chloro-5,12-dihydroquinoxalino[2,3-*b*]quinoxaline skeleton and to evaluate the influence of the “heavy atom” on the ability to initiate photo-oxidizable sensitization systems. These systems include: the collection of dyes, **4a–4f**, and initiators (Scheme 4), such as N-methoxy-4-phenylpyridinium tetrafluoroborate (**5**), N-ethoxy-2-methylpyridinium hexafluorophosphate (**6**) and diphenyliodonium hexafluorophosphate (**7**). The initiation ability of dyes mentioned above, **4a–4f**, was compared with the initiation ability of dye **4g**, which does not contain halogens in its structure. This paper also reports on the spectroscopic, photophysical, and electrochemical properties of these visible-light sensitizers. Finally, experimental results show that these new photooxidizable sensitization systems could be used as visible-light photoinitiators for the free radical polymerization of acrylate or for the cationic polymerization of epoxide monomers. In our studies we choose trimethylolpropane triacrylate (**8**) as the multifunctional acrylate monomer. The cyclohexene oxide (**9**) was chosen as epoxide, which cannot be polymerized by a radical mechanism. The structure of synthesized dyes, initiators and monomers are presented in Scheme 4.

2. Experimental

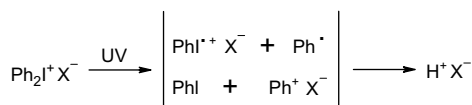
2.1. General

5, **7**, monomers (**8**, **9**) and the necessary synthesis reagents were purchased from Sigma – Aldrich (Poznan, Poland). **6** was synthesized according to the procedure described in Ref. [13]. The quinoxalines (**2a–3c**) and dyes **4a–4g** were identified and characterized via ^1H NMR spectroscopy [Bruker Avance DPX 250, DMSO- d_6 , TMS standard, δ (ppm)]. Their purity was confirmed using TLC [Merck Silica gel 60, solvent: 3:1 (v/v) toluene/pyridine]. The chemical ionization mass spectra were recorded on a Finnigan MAT 94 spectrometer with isobutane application. Absorption and steady-state fluorescence spectra were recorded using a Lambda 40 spectrophotometer (Perkin Elmer, USA) and a FluoroLog 3 spectrofluorimeter (Horiba Jobin Yvon, USA), respectively.

2.2. Synthesis

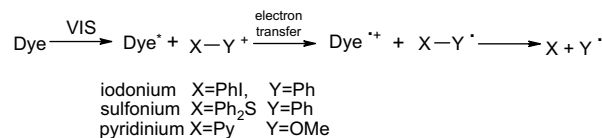
2.2.1. Synthesis of 6-bromo-1,4-dihydroquinoxaline-2,3-dione (**2b**)

4-Bromo-1,2-phenylenediamine (7.71 g, 0.04 mol) and oxalic acid (5.04 g, 0.04 mol) were refluxed in hydrochloric acid (30%, 40 ml) for 3 h. After cooling, the resulting light violet precipitate



$\text{X}^- = \text{PF}_6^-, \text{SbF}_6^-, \text{AsF}_6^-, \text{etc.}$

Scheme 2.



Scheme 3.

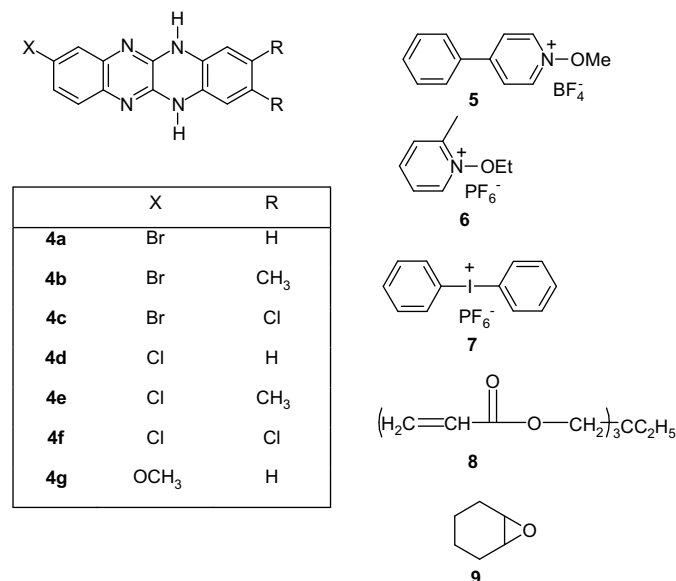
was filtered and washed with water to yield **2b** (8.83 g, 92%, m.p. > 360 °C). **2b** was carried on to the next step of the synthesis without purification. **2a** and **2c** 1,4-dihydroquinoxaline-2,3-diones were synthesized, in a similar fashion, from 4-chloro-1,2-phenylenediamine and 4-methoxy-1,2-phenylenediamine starting material, respectively. Table 1 presents the yield, melting point and ^1H NMR data for compounds **2a–2c**.

2.2.2. Synthesis of 6-bromo-2,3-dichloroquinoxaline (**3b**) [14]

DMF was added dropwise (0.5 ml) to a solution of **2b** (6.0 g, 0.025 mol) in thionyl chloride (120 ml). The reaction mixture was refluxed for 20 h and then concentrated under vacuum. The resulting residue was coevaporated with chloroform several times, dissolved in chloroform (100 ml), and poured over ice-water. The organic layer was collected, washed with saturated aqueous NaCl, dried over Na_2SO_4 , and then evaporated to provide **3b** as a brown solid (3.61 g, 52%). **3b** was used for the next step in the synthesis without further purification. 2,3,6-Trichloroquinoxaline (**3a**) and 6-methoxy-2,3-dichloroquinoxaline (**3c**) were synthesized in the same manner from the **2a** and **2c** substrates, respectively. Table 1 presents the yield, melting point and ^1H NMR data for quinoxaline compounds **3a–3c**.

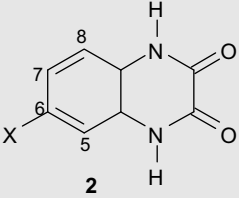
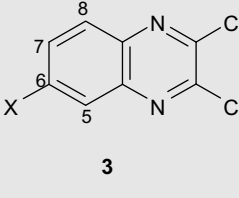
2.2.3. Synthesis of 8-bromo-5,12-dihydroquinoxalino[2,3-*b*]quinoxaline (**4d**)

6-Bromo-2,3-dichloroquinoxaline (1.2 g, 0.0043 mol) and *o*-phenylenediamine (0.93 g, 0.0086 mol) were refluxed in ethylene glycol (10 ml) for 30 min. After cooling, the yellow precipitate was filtered, washed with methanol, dried, and recrystallized from acetic acid. The product (1.15 g) was obtained with an 86% yield. The other dyes were synthesized in the same manner, from the appropriate *o*-phenylenediamines. Table 2 presents the yield, melting point, elemental analysis, ^1H NMR and CI MS data for these dyes.



Scheme 4.

Table 1
Melting point, yield and ^1H NMR spectra of quinoxalines (**2a–3c**).

Compound	M.p. [$^{\circ}\text{C}$]	Yield [%]	^1H NMR J [Hz]; δ [ppm]	
				  2 3
2a	>360 (>350 [15])	92	7.02–7.11 (m, 1H, H7), 7.21–7.26 (m, 2H, H5, H8), 11.95 (d, 2H, J = 7.5, NH)	
2b	>360	95	7.08–7.13 (m, 3H, H5, H7, H8), 11.96 (d, 2H, J = 5, NH)	
2c	342–344	89	3.70 (s, 3H, OCH ₃), 6.66–6.72 (m, 2H H5, H7), 7.02 (d, 1H, J = 7.5, H8), 11.78 (d, 2H, J = 12.5, NH)	
3a	130–131 (132 [16])	78	7.98–8.10 (m, 2H, H7, H8), 8.27–8.28 (m, 1H, H5)	
3b	140–141 (141–142 [17])	64	7.73–7.78 (m, 1H, H7), 7.96–8.03 (m, 2H, H5, H8)	
3c	131–133	99	3.96 (s, 3H, OCH ₃), 7.41–7.46 (m, 1H, H7), 7.88–7.99 (m, 2H, H5, H8)	

2.3. Photochemical experiments

All photochemical experiments were carried out in a Rayonet Reactor RPR 200 (Southern New England Ultraviolet Co, USA) equipped with eight lamps emitting light at 419 nm. Illumination intensity was measured using uranyl oxalate actinometry [18].

The fluorescence quantum yield of the dye (Φ_{dye}) was calculated from the following equation:

$$\Phi_{\text{dye}} = \Phi_{\text{ref}} I_{\text{dye}} A_{\text{ref}} n_{\text{dye}}^2 / I_{\text{ref}} A_{\text{dye}} n_{\text{ref}}^2 \quad (1)$$

in which Φ_{ref} denotes the fluorescence quantum yield of the 5,12-dihydroquinoxalino[2,3-*b*]quinoxaline reference ($\Phi_{\text{ref}} = 0.8$ in 1-methyl-2-pyrrolidone [11]), A_{dye} and A_{ref} denote the absorbances of the dye and the reference (at the 410 nm excitation wavelength), I_{dye} and I_{ref} refer to the areas under the fluorescence peaks of the dye and reference, and n_{dye} and n_{ref} are the solvent refractive indices for the dye and reference, respectively.

In all polymerization experiments a cut-off filter was used to eliminate wavelengths lower than 400 nm. Free radical photopolymerization reactions were conducted in solvent mixture of 1 ml of 1-methyl-2-pyrrolidone (MP) and 4 ml of trimethylolpropane triacrylate. The concentrations of dye and N-alkoxy-pyridinium salts (**5**, **6**) were maintained at 0.1 mM and 10 mM, respectively. The solutions were degassed prior to the experiments by bubbling with N_2 for 10 min and they were irradiated for 120 s. The rate of polymerization (R_p) and the double bond conversion (p) were calculated from Eqs. (2) and (3), respectively:

$$R_p = Q_s M / n \Delta H_p m \quad (2)$$

$$p = (\Delta H_t / n \Delta H_p) \times 100\% \quad (3)$$

In these expressions, Q_s is heat flow per second during the reaction, m is the mass of the monomer in the sample, M is the molar mass of the monomer, n is the number of double bonds per monomer, ΔH_t is the heat generated during 120 s of irradiation, and ΔH_p is the theoretical enthalpy for complete polymerization of acrylate double bonds (20.6 kcal/mol) [19]. The heat flow was measured with a PT 401 temperature sensor (Elmetron, Poland), immersed in the sample. A polymerizing mixture containing the dye without a pyridinium salt was used as a reference sample.

Cationic photopolymerization of cyclohexene oxide (5 ml) was conducted under an N_2 atmosphere. The concentrations of dye and diphenyliodonium salt (**7**) were 0.1 mM and 10.0 mM, respectively. The cyclohexene oxide was polymerized using a 30-min exposure to radiation, and the resulting solution was poured into 50 ml of methanol containing roughly 1 ml of NH_3 (30%). The precipitated

polymers were isolated by filtration, washed with cold methanol, and dried overnight in a vacuum oven at 45°C . The conversion of cyclohexene oxide into polymer was then determined gravimetrically.

3. Results and discussion

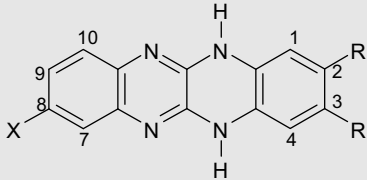
3.1. Synthesis and spectroscopic characterization of dyes

The synthesis of the collection of dyes, **4**, is outlined in Scheme 5. In the first step, the corresponding 4-halogeno-1,2-phenylenediamines (**1a–1b**) or 4-methoxy-1,2-phenylene-diamines (**1c**) were cyclized with oxalic acid in refluxing hydrochloric acid (30%). This produced the derivatives, 6-halogeno-1,4-dihydroquinoxaline-2,3-dione (**2a–2b**) or 6-methoxy-1,4-dihydroquinoxaline-2,3-dione (**2c**), in $\sim 90\%$ yield. The chlorination of **2**, by treatment with thionyl chloride, created derivatives of chloroquinoxalines (**3a–3c**) [14], in $\sim 70\%$ yield. Finally, dyes **4a–4g** were synthesized by refluxing **3a–3c** with the appropriate symmetric *o*-phenylenediamines, in ethylene glycol.

The crude dyes were recrystallized from acetic acid, until a constant molar excitation coefficient and TLC purity were obtained. Dyes **4a–4g** were synthesized at 64–86% yield, and their chemical structures were verified by elemental analysis, ^1H NMR and CI MS spectra (Table 2). The spectroscopic properties (absorption and fluorescence) of dyes **4a–4g** are presented in Table 3. Dyes **4a–4g** had absorption bands in the visible region, located at approximately 420 nm, and emission bands located at approximately 480 nm characterized by a ~ 62 –80 nm Stokes shift. These values indicate that the geometry of the singlet excited state does not differ greatly from the geometry of the ground state. The electronic absorption (UV–vis) and emission spectra of dye **4d** are presented in Fig. 1. For all dyes tested, the absorption and fluorescence spectra were nearly mirror images of each other, with overlapping bands corresponding to the $0 \rightarrow 0$ transition. The absorption spectra were typical for polycyclic aromatic heterocycles, which have a characteristic vibrational structure. In comparison with 5,12-dihydroquinoxalino[2,3-*b*]quinoxaline [11], the presence of an additional halogen atom in dyes **4a** and **4d** had no effect on the position of the absorption bands. The examined dyes exhibited small solvatochromic effects. The bathochromic shift between nonpolar solvent (cyclohexene oxide, $\epsilon \sim 9$) and polar solvents (1-methyl-2-pyrrolidone, $\epsilon = 33$) of 2–4 nm was observed.

The fluorescence quantum yields (Φ_f) of the dyes are presented in Table 3. The Φ_f of these dyes range from 0.24 to 0.92, with dyes **4a–4c** having the smallest values of Φ_f . Adding heavy

Table 2
Melting point, yield, R_f and ^1H NMR spectra of dyes **4a–4g**.

Dye	M.p. [°C]	Yield [%]	Elemental analysis	MS Cl m/z	R_f	^1H NMR J [Hz]; δ [ppm]
						
4a	>360	86	Anal. Calcd for $\text{C}_{14}\text{H}_9\text{N}_4\text{Br}$ C, 53.70; H, 2.90; N, 17.89 Found: C, 53.4; H, 2.8; N, 17.8	$M = 313.1$ 312.0 $[\text{M} - \text{H}]^+$, 313.0 $[\text{M}]^+$ 314.0 $[\text{M} + \text{H}]^+$, 315.0 $[\text{M} + 2\text{H}]^+$ 235.1 $[\text{M} + 2\text{H} - \text{Br}]^+$	0.85	6.90–7.06 (m, 5H, H1, H2, H3, H4, H10), 7.15–7.20 (m, 2H, H7, H9), 10.14 (bs, 2H, NH)
4b	322–324	75	Anal. Calcd for $\text{C}_{16}\text{H}_{13}\text{N}_4\text{Br}$ C, 56.32; H, 3.84; N, 16.42 Found: C, 56.0; H, 3.9; N, 16.5	$M = 341.2$ 340.1 $[\text{M} - \text{H}]^+$, 341.1 $[\text{M}]^+$ 342.1 $[\text{M} + \text{H}]^+$, 343.1 $[\text{M} + 2\text{H}]^+$ 263.2 $[\text{M} + 2\text{H} - \text{Br}]^+$	0.79	1.90 (s, 3H, CH_3), 2.49 (s, 3H, CH_3), 6.53–6.71 (m, 3H, H1, H4, H10), 6.83–6.89 (m, 2H, H7, H9), 7.35 (s, 2H, NH)
4c	331–332	65	Anal. Calcd for $\text{C}_{14}\text{H}_7\text{N}_4\text{BrCl}_2$ C, 44.01; H, 1.85; N, 14.66 Found: C, 44.1; H, 1.9; N, 14.7	$M = 382.1$ 380.9 $[\text{M} - \text{H}]^+$, 381.9 $[\text{M}]^+$ 382.9 $[\text{M} + \text{H}]^+$, 347.0 $[\text{M} - \text{Cl}]^+$ 303.0 $[\text{M} + \text{H} - \text{Br}]^+$	0.81	6.45–6.87 (m, 3H, H1, H4, H10), 7.30 (s, 2H, H7, H9), 10.25 (s, 2H, NH)
4d	>360	84	Anal. Calcd for $\text{C}_{14}\text{H}_9\text{N}_4\text{Cl}$ C, 62.58; H, 3.37; N, 20.85 Found: C, 62.7; H, 3.5; N, 20.9	$M = 268.7$ 268.1 $[\text{M}]^+$, 269.1 $[\text{M} + \text{H}]^+$, 270.1 $[\text{M} + 2\text{H}]^+$, 235.1 $[\text{M} + 2\text{H} - \text{Cl}]^+$	0.85	6.70–7.05 (m, 7H, H1, H2, H3, H4, H7, H9, H10), 10.04 (s, 2H, NH)
4e	335–336	67	Anal. Calcd for $\text{C}_{16}\text{H}_{13}\text{N}_4\text{Cl}$ C, 64.76; H, 4.41; N, 18.88 Found: C, 64.8; H, 4.5; N, 18.9	$M = 296.8$ 296.1 $[\text{M}]^+$, 297.1 $[\text{M} + \text{H}]^+$, 263.1 $[\text{M} + 2\text{H} - \text{Cl}]^+$	0.78	2.06 (s, 6H, CH_3), 6.31–7.03 (m, 4H, H1, H4, H9, H10), 7.35 (s, 1H, H7), 9.91 (s, 2H, NH)
4f	346–347	65	Anal. Calcd for $\text{C}_{14}\text{H}_7\text{N}_4\text{Cl}_3$ C, 49.81; H, 2.09; N, 16.60 Found: C, 49.9; H, 2.2; N, 16.7	$M = 337.6$ 336.1 $[\text{M} - \text{H}]^+$, 337.1 $[\text{M}]^+$ 338.1 $[\text{M} + \text{H}]^+$, 343.1 $[\text{M} + 2\text{H}]^+$, 302.1 $[\text{M} - \text{Cl}]^+$	0.79	6.69–6.83 (m, 3H, H1, H4, H10), 6.93 (s, 2H, H7, H9), 11.22 (s, 2H, NH)
4g	>360	60	Anal. Calcd for $\text{C}_{15}\text{H}_{12}\text{N}_4\text{O}$ C, 68.17; H, 4.57; N, 21.20 Found: C, 68.3; H, 4.7; N, 21.3	$M = 264.3$ 264.1 $[\text{M}]^+$, 265.1 $[\text{M} + \text{H}]^+$	0.70	3.69 (s, 3H, OCH_3), 6.45–6.69 (m, 6H, H1, H2, H3, H4, H7, H9), 6.82–6.86 (m, 1H, H10), 10.50–11.60 (bs, 2H, NH)

atoms, such as Br, to a fluorescent system is known to stabilize a molecule's triplet state by increasing the efficiency of the intersystem crossing process. To clarify the photochemistry of dyes **4a–4f**, their quantum yields of singlet oxygen generation [$\Phi(^1\text{O}_2)$] were measured in an oxygen-saturated solution (Table 3). Additionally, dye **4g** was synthesized without halogen; the dye's ability to generate singlet oxygen was measured. In accordance with the aforementioned "heavy atom effects", the quantum yield of singlet oxygen generation was much greater for the dyes derived from 6-bromo-2,3-dichloroquinoxaline. Moreover, the smallest $\Phi(^1\text{O}_2)$ was for dye **4g**, which did not contain any halogen atoms.

3.2. Sensitized free radical and cationic photopolymerization

Spectroscopic studies revealed that dyes **4a–4g** could be applied as visible sensitizers for light >400 nm. Generally accepted mechanism of the dye-sensitized photodecomposition of pyridinium and iodonium salts [5–7] is presented in Scheme 3. Irradiation of these photoredox pairs leads to electron transfer from the excited sensitizer (Dye^*) to the pyridinium/iodonium salt (X-Y^+). The resulting radical (X-Y^\cdot) is then cleaved to yield the initiator radical ($^\cdot\text{Y}$), sensitizer radical cation ($\text{Dye}^{+\cdot}$), and neutral molecule, X. N-alkoxy pyridinium salt cleavage yields pyridine and an alkoxy radical, while diphenyliodonium salt cleavage yields iodobenzene and a phenyl radical. The rapid decomposition of the initiator radical retards back electron-transfer and renders the overall process irreversible.

Table 3

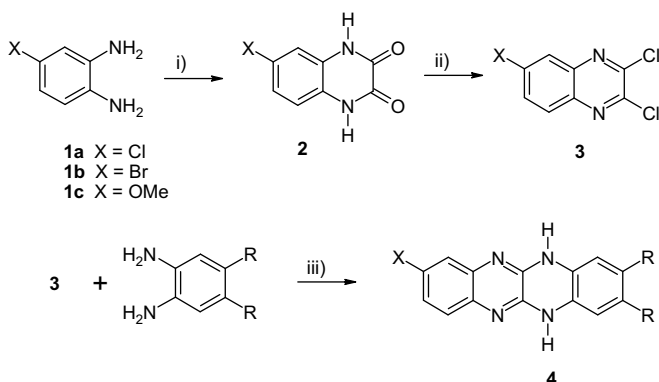
Spectroscopic, photophysical, and electrochemical parameters of the examined dyes.

Dye	λ_{max}^a [nm]	ϵ^a [dm ³ mol ^{−1} cm ^{−1}]	λ_{max}^b [nm]	λ_{fl}^b [nm]	Φ_{fl}^b	Stokes Shift [nm]	$\Phi(^1\text{O}_2)^a$	E^{00} [kJ mol ^{−1}]	E_{ox} [V] ^c
4a	418	24,050	416	479	0.24	63	0.60	270	0.42
4b	417	21,200	413	493	0.36	80	0.63	263	0.38
4c	420	23,170	418	482	0.28	64	0.58	268	0.52
4d	418	25,910	416	478	0.89	62	0.30	283	0.42
4e	417	25,670	413	492	0.88	79	0.36	265	0.37
4f	420	24,100	417	481	0.88	64	0.43	269	0.51
4g	421	26,600	418	480	0.90	62	0.08	269	0.29

^a In 1-methyl-2-pyrrolidone.

^b In cyclohexene oxide.

^c In DMF.



Scheme 5. i) Oxalic acid, 30% HCl; ii) SOCl_2 , DMF; iii) Ethylene glycol.

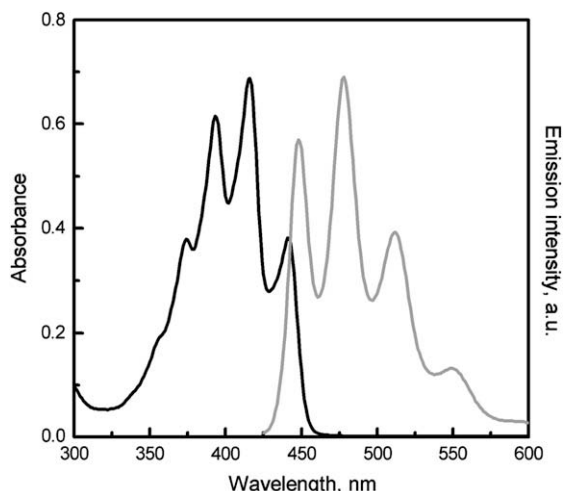


Fig. 1. Normalized absorption (black) and emission (gray) spectra of dye **4d** (1.45 μM) in cyclohexene oxide.

The free energy change in photoinduced electron transfer from the excited dyes **4a–4g** to the initiators, was calculated from the Rehm–Weller equation [20]:

$$\Delta G_{\text{et}} (\text{kJ mol}^{-1}) = 97 [E_{\text{ox}}(S/S^{*+}) - E_{\text{red}}(A^{\cdot-}/A)] - E^{00}(S) - Z_1 Z_2 / \epsilon r_{12} \quad (4)$$

In this equation, $E_{\text{ox}}(S/S^{*+})$ and $E_{\text{red}}(A^{\cdot-}/A)$ are the oxidation potential of dyes **4** and the reduction potential of the pyridinium/iodonium salt, respectively. The $E^{00}(S)$ is the singlet excited state energy of dyes **4**, which is given in Table 3. The last term represent the Coulombic energy necessary to form an ion pair with charge Z_1 and Z_2 in a medium of dielectric constant ϵ for a distance r_{12} . In the present case, since in the electron transfer process the neutral radical of the pyridinium/iodonium compound is formed ($Z=0$), this term is negligible.

In order to calculate ΔG_{et} , the oxidation potentials of dyes **4** were measured in different experiments. The cyclic voltammogram of dye **4b** is presented in Fig. 2, and the measured oxidation potentials (E_{ox}) of all of the dyes are presented in Table 3. In all cases, the electrochemical oxidation was irreversible, and the location of the oxidation peak depended on the structure of the dye. The results indicated that dye **4g**, which contains a methoxy group, is oxidized

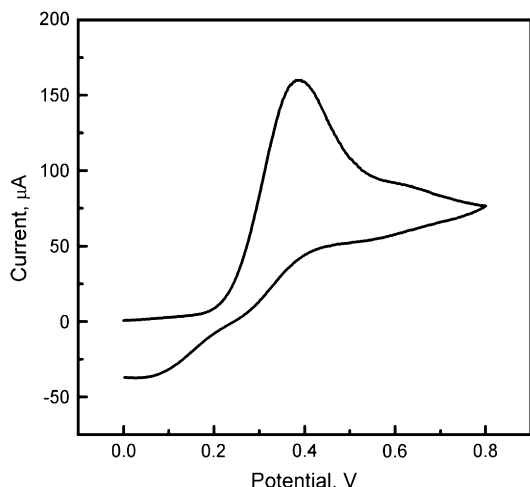


Fig. 2. Cyclic voltammograms of dye **4b** in DMF. Scan rate: 0.1 V s^{-1} .

Table 4
Thermodynamic data (kJ mol^{-1}).

Dye	ΔG_{et}		
	$5^+ E_{\text{red}} = -1.02$	$6^+ E_{\text{red}} = -1.22$	$7 E_{\text{red}} = -0.97$
4a	−130.3	−110.9	−135.2
4b	−127.2	−107.8	−132.1
4c	−118.6	−99.2	−123.5
4d	−143.3	−123.9	−148.2
4e	−130.2	−110.8	−135.0
4f	−120.6	−101.2	−125.4
4g	−141.9	−122.5	−146.8

From Ref. [21].

at the lowest potential. Moreover, dyes with two methyl groups (**4b** and **4e**) are more readily oxidized than unsubstituted dyes (**4a** and **4d**) and halogen-substituted analogues (**4c** and **4f**).

Once the E_{ox} and E^{00} values of dyes **4**, and the reduction potential of the initiators (**5–7**) had been measured, the ΔG_{et} could be calculated using Eq. (4). The calculated thermodynamic parameters, listed in Table 4, indicated that all the tested dye/initiator systems possessed a highly favorable thermodynamic driving force upon exposure to light ($-\Delta G_{\text{et}} > 99 \text{ kJ mol}^{-1}$). This meant that the excited-state photoelectron transfer was quite facile.

Finally, the dye/pyridinium photoredox pairs were examined for potential applications as initiators for the free radical polymerization of trimethylolpropane triacrylate monomer. Different techniques have been applied to study the kinetics of polymerization reaction. According to the measurement two kinds of methodologies have been used: (i) direct based on the determination of polymer formed or residual monomer and (ii) indirect, that measures the change of a property of the system during polymerization (e.g. density, heat flow) [22]. The rate of radical induced polymerization results in large heat flow, therefore the efficiency of the polymerization, initiated by the **4/5** and **4/6** systems, was measured indirectly from the reaction's heat flow during irradiation (Fig. 3). The overall polymerization results are summarized in Table 5.

The calculated polymerization rate (R_p) and double bond conversion (p), presented in Table 5, indicated that the efficiency of polymerization strongly depended upon the structure of the dye

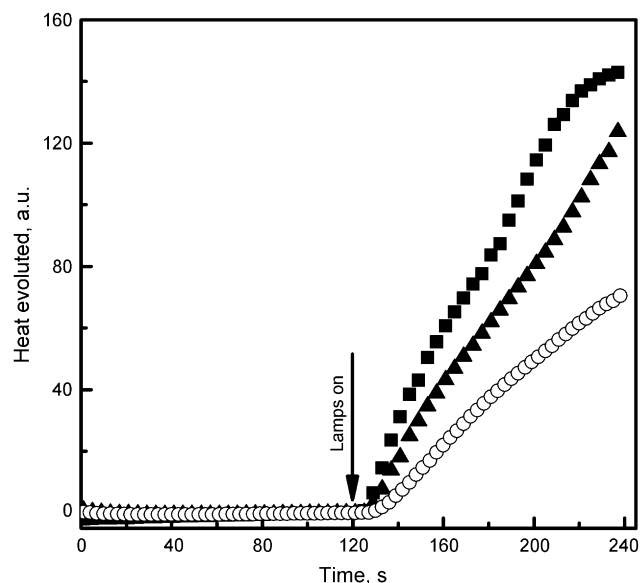


Fig. 3. Kinetic curves of **8** photopolymerization recorded under a N_2 atmosphere for **5** and dyes **4b** (■), **4c** (▲) and **4g** (○).

Table 5

Rate of photopolymerization ($\mu\text{mol s}^{-1}$) of **8**, conversion (%) of monomers and quantum yield of acid release (mmol quant^{-1}).

Dye	8⁺				9⁺	MP⁺	
	5		6				7
	<i>R</i> _p	%	<i>R</i> _p	%			
4a	37.55	26	33.52	24	97	52.6	
4b	38.92	28	29.88	21	73	32.6	
4c	34.55	25	29.79	21	85	27.9	
4d	15.74	11	18.06	13	63	11.7	
4e	20.55	15	22.80	16	39	6.7	
4f	29.74	21	25.34	18	62	9.0	
4g	9.62	2	5.31	1	29	4.5	

^{*} N_2 atmosphere.

employed. Dyes **4a–4c** significantly accelerated triacrylate photopolymerization. As shown in Eq. (5), the rate of the photoinitiated polymerization depends on the efficiency of forming an excited triplet state [23]:

$$R_p = k_p[M](I_a\Phi_T k_{el}k_t)^{0.5} \quad (5)$$

where I_a is the intensity of the absorbed light, Φ_T is the quantum yield of triplet state formation, k_p and k_t denote the rate constants of polymerization and chain termination steps, respectively, and k_{el} is the first-order rate constant of the electron transfer. The relationship between R_p and the square root of $\Phi(^1\text{O}_2)$ (Fig. 4) revealed the possibility that the electron transfer between dyes and pyridinium salt occurs via the triplet state [11,12,23].

Dye **4/7** photoredox pairs were also examined for their usefulness as photoinitiators for the cationic polymerization of cyclohexene oxide. For these experiments, polymerization was conducted under a N_2 atmosphere, and the reaction mixture was irradiated for 30 min. The details regarding the conversion of cyclohexene oxide into polymer are presented in Table 5. It was evident that dyes **4a–4c** significantly accelerated cyclohexene oxide polymerization.

Protic acids can be used to initiate cationic polymerization reactions [4–6,9,10,12]. To confirm the formation of the acid during photolysis of the **4/7** systems, the quantum yield of acid release [$\Phi(\text{H}^+)$] upon photolysis was measured using sodium bromophenol blue (**BPhBI**). The quantity of acid released was estimated by comparison with a calibration curve of the **BPhBI** absorbance as

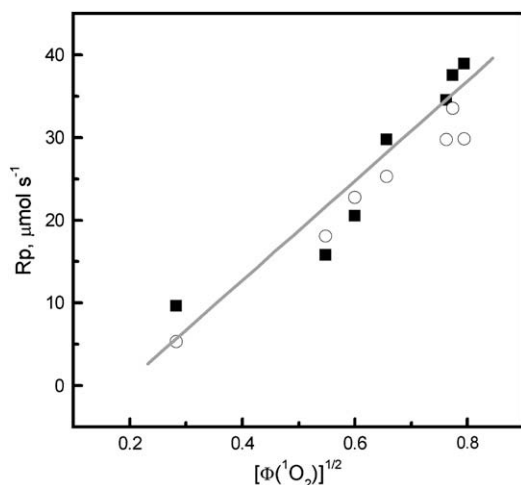


Fig. 4. Relationship between the rate of polymerization, initiated by dye/**5** (■) and dye/**6** (○) systems, and the square root of quantum yield of singlet oxygen formation ($R = 0.95$).

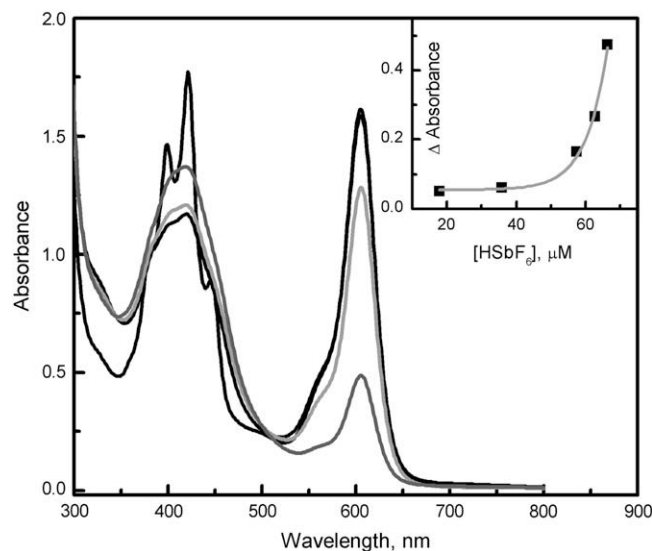


Fig. 5. Electronic absorption spectra obtained upon photolysis (time interval, 10 s) of a N_2 -saturated solution of **BPhBI** (10 μM) and dye **4c** (0.1 mM)/**7** (10.0 mM) system in 1-methyl-2-pyrrolidone. Inset: calibration curve for the change in **BPhBI** (10 μM) absorbance vs. HSbF_6 concentration (range 0–70 μM).

a function of HSbF_6 concentration (inset Fig. 5). In all the dye/**7** combinations studied, the solution acidity increased with irradiation time, whereas the solution's **BPhBI** absorbance at λ_{max} (606 nm) decreased correspondingly (Fig. 5). In contrast, the solution pH would not change if the dyes are photolyzed in the absence of the salt. The calculated quantum yields of acid release are presented in Table 5. Dye **4a** demonstrated the highest quantum yield of acid release. Moreover, there was a linear relationship between $\Phi(\text{H}^+)$ and the conversion of cyclohexene oxide (Fig. 6). This suggests that the proton, formed upon photolysis of the **4/7** systems, is the crucial species for initiating the cationic polymerization of cyclohexene oxide.

Dyes **4a–4c** significantly accelerated the photopolymerization of triacrylate and epoxide monomers. These compounds also demonstrated the highest quantum yields of singlet oxygen generation (Table 3). The relationships between the square root of $\Phi(^1\text{O}_2)$ and both the rate of free radical polymerization and $\Phi(^1\text{O}_2)$ and the conversion of cyclohexene oxide, revealed that the oxidation of dyes **4a–4f** may occur via the triplet state [11,12,23].

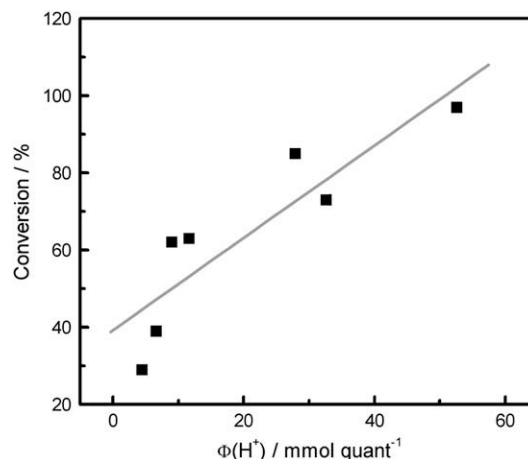


Fig. 6. Relationship between the conversion of **9** and the quantum yield of acid release ($R = 0.9$).

4. Conclusions

Novel dyes based on the 8-halogeno-5,12-dihydroquinoxalino[2,3-*b*]quinoxaline skeleton were successfully synthesized and characterized using ^1H NMR and CI MS spectroscopy. These new dyes, when combined with salts, such as N-methoxy-4-phenylpyridinium tetrafluoroborate (**5**), N-ethoxy-2-methylpyridinium hexafluorophosphate (**6**) or diphenyliodonium hexafluorophosphate (**7**), may have practical applications as visible-light photoinitiators for free radical and/or cationic polymerization. The ability of each dye to act as a photoinitiator strongly depended upon its chemical structure. Furthermore, the heavy atoms present in dyes **4a–4f** could promote the formation of the dyes' excited triplet states, thereby facilitating electron transfer from these states.

Acknowledgements

This work was supported by the Polish Ministry of Science and Higher Education (project no. N N205 1454 33)

References

- [1] Fouassier JP. In: Fouassier JP, Rabek JF, editors. Radiation curing in polymer science and technology: fundamentals and methods, vol. I. London: Elsevier; 1993. p. 49–113.
- [2] Koleske JV. Radiation curing of coatings. West Conshohocken: ASTM International; 2002. 211–232.
- [3] Allen NS. Photoinitiators for UV and visible curing of coatings: mechanisms and properties. *J Photochem Photobiol A Chem* 1996;100:101–9.
- [4] Crivello JV. The discovery and development of onium salt cationic photoinitiators. *J Polym Sci A Polym Chem* 1999;37:4241–54.
- [5] Selvaraju C, Sivakumar A, Ramamurthy P. Excited state reactions of acridine-dione dyes with onium salts: mechanistic details. *J Photochem Photobiol A Chem* 2001;138:213–26.
- [6] Neumann MG, Rodriques MR. A study of the elemental reactions involved in the initiation of the polymerization of tetrahydrofuran induced by the photosensitization of a triphenylsulphonium salt by perylene. *J Braz Chem Soc* 2003;14:76–82.
- [7] Gould IR, Shukla D, Giesen D, Farid S. Energetics of electron-transfer reactions of photoinitiated polymerization: dye-sensitized fragmentation of N-alkoxy-pyridinium salts. *Helv Chim Acta* 2001;84:2796–812.
- [8] Timpe HJ, Ulrich S, Decker C, Fouassier JP. Photoinitiated polymerization of acrylates and methacrylates with decahydroacridine-1,8-dione/onium salt initiator systems. *Macromolecules* 1993;26:4560–6.
- [9] Zhu QQ, Schnabel W. Cationic photopolymerization under visible laser light: polymerization of oxiranes with coumarin/onium salt initiator systems. *Polymer* 1996;37:4129–33.
- [10] Crivello JV, Bulut U. Curcumin: a naturally occurring long-wavelength photosensitizer for diaryliodonium salts. *J Polym Sci A Polym Chem* 2005;43:5217–31.
- [11] Podsiadly R. Photoreaction and photopolymerization studies on fluoquinolone dye-pyridinium salt systems. *J Photochem Photobiol A Chem* 2008;198:60–8.
- [12] Podsiadly R. The synthesis of novel, visible-wavelength oxidizable polymerization sensitizers based on the 5,12-dihydroquinoxalino[2,3-*b*]pyridopyrazine skeleton. *Dyes Pigments* 2009;80:86–92.
- [13] Reichardt C. Notiz zur Darstellung von N-Äthoxy-pyridinium- und -chinolinium salzen. *Chem Ber* 1966;97:1769–70.
- [14] Ohmori J, Shimizu-Sasamata M, Okada M, Sakamoto S. 8-(1*H*-Imidazol-1-yl)-7-nitro-4(5*H*)-imidazo[1,2-*a*]quinoxaline and related compounds: synthesis and structure-activity relationships for the AMPA-type non-NMDA receptor. *J Med Chem* 1997;40:2053–63.
- [15] Ahmad Y, Habib MS, Iqbal M, Ziauddin. Quinoxaline derivatives. V. Some reactions of 2-cyano-3-hydroxyquinoxaline 1-oxide. *Bull Chem Soc Jpn* 1965;38:562–5.
- [16] Lanquist JK. Quinoxaline N-oxides. Part I. The oxidation of quinoxalines and its Bz-substituted derivatives. *J Chem Soc* 1953:2816–9.
- [17] Cheeseman GWH. Quinoxalines and related compounds. Part VI. Substitution of 2,3-dihydroxyquinoxaline and its 1,4-dimethyl derivative. *J Chem Soc* 1962:1170–5.
- [18] Leighton WB, Forbes GS. Precision actinometry with uranyl oxalate. *J Am Chem Soc* 1930;52:3139–52.
- [19] Avci D, Nobles J, Mathias LJ. Synthesis and photopolymerization kinetics of new flexible diacrylate and dimethacrylate crosslinkers based on C18 diacid. *Polymer* 2003;44:963–8.
- [20] Rehm D, Weller A. Kinetics of fluorescence quenching by electron and H-atom transfer. *Isr J Chem* 1970;8:259–71.
- [21] Schnabel W. Cationic photopolymerization with the aid of pyridinium-type salts. *Macromol Rapid Commun* 2000;21:628–42.
- [22] Rabek JF. In: Fouassier JP, Rabek JF, editors. Radiation curing in polymer science and technology: fundamentals and methods, vol. I. London: Elsevier; 1993. p. 329–452.
- [23] Przyjazna B, Kucybała Z, Pączkowski J. Development of new dyeing photoinitiators based on 6*H*-indolo[2,3-*b*]quinoxaline skeleton. *Polymer* 2004;45:2559–66.